5-22-2023

Néel Spin Currents in Antiferromagnets

Ding-Fu Shao

Yuan-Yuan Jiang

Jun Ding

Shu-Hui Zhang

Zi-An Wang

See next page for additional authors

Authors

Ding-Fu Shao, Yuan-Yuan Jiang, Jun Ding, Shu-Hui Zhang, Zi-An Wang, Rui-Chun Xiao, Gautam Gurung, W. J. Lu, Y. P. Sun, and Evgeny Y. Tsymbal

Néel Spin Currents in Antiferromagnets

Ding-Fu Shao,[1,*,†] Yuan-Yuan Jiang,[1,2,*] Jun Ding,[3,*] Shu-Hui Zhang,[4] Zi-An Wang,[1,2] Rui-Chun Xiao,[5] Gautam Gurung,[6] W. J. Lu,[1] Y. P. Sun,[7,1,8] and Evgeny Y. Tsymbal[9,‡]

[1]*Key Laboratory of Materials Physics, Institute of Solid State Physics, HFIPS, Chinese Academy of Sciences, Hefei 230031, China*

[2]*University of Science and Technology of China, Hefei 230026, China*

[3]*College of Science, Henan University of Engineering, Zhengzhou 451191, People's Republic of China*

[4]*College of Mathematics and Physics, Beijing University of Chemical Technology, Beijing 100029, People's Republic of China*

[5]*Institute of Physical Science and Information Technology, Anhui University, Hefei 230601, China*

[6]*Trinity College, University of Oxford, Broad Street, Oxford, OX1 3BH, United Kingdom*

[7]*High Magnetic Field Laboratory, HFIPS, Chinese Academy of Sciences, Hefei 230031, China*

[8]*Collaborative Innovation Center of Microstructures, Nanjing University, Nanjing 210093, China*

[9]*Department of Physics and Astronomy & Nebraska Center for Materials and Nanoscience, University of Nebraska, Lincoln, Nebraska 68588-0299, USA*

(Received 12 December 2022; accepted 19 April 2023; published 22 May 2023)

Ferromagnets are known to support spin-polarized currents that control various spin-dependent transport phenomena useful for spintronics. On the contrary, fully compensated antiferromagnets are expected to support only globally spin-neutral currents. Here, we demonstrate that these globally spin-neutral currents can represent the Néel spin currents, i.e., staggered spin currents flowing through different magnetic sublattices. The Néel spin currents emerge in antiferromagnets with strong intrasublattice coupling (hopping) and drive the spin-dependent transport phenomena such as tunneling magnetoresistance (TMR) and spin-transfer torque (STT) in antiferromagnetic tunnel junctions (AFMTJs). Using RuO_2 and Fe_4GeTe_2 as representative antiferromagnets, we predict that the Néel spin currents with a strong staggered spin polarization produce a sizable fieldlike STT capable of the deterministic switching of the Néel vector in the associated AFMTJs. Our work uncovers the previously unexplored potential of fully compensated antiferromagnets and paves a new route to realize the efficient writing and reading of information for antiferromagnetic spintronics.

DOI: 10.1103/PhysRevLett.130.216702

Over decades, ferromagnetic metals have been intensively explored and widely employed in spintronics [1]. Ferromagnets intrinsically support spin-polarized currents, which drive spin-dependent transport phenomena such as tunneling magnetoresistance (TMR) [2–4] and spin-transfer torque (STT) [5–7] in magnetic tunnel junctions (MTJs), crucial for electrical writing and reading of information that is stored in the magnetization orientation [8].

Recently, antiferromagnets have emerged as an alternative of ferromagnets for spintronic applications [9–12]. Because of being robust against magnetic perturbations, not producing stray fields, and exhibiting ultrafast spin dynamics, antiferromagnets may potentially overperform ferromagnets. However, reading and writing information using an antiferromagnetic (AFM) Néel vector as a state variable appear to be more challenging. Because of the absence of a net magnetization, spin-polarized currents and hence TMR and STT are not expected to occur in AFM systems.

In the past decade, significant progress has been achieved in the understanding of electronic and transport properties of antiferromagnets [13–20], resulting in discoveries of the spin-orbit torques [21–25], the linear [26–30] and nonlinear [31–35] anomalous Hall effects, the Néel vector dependent spin currents [36–49], and TMR in AFM tunnel junctions (AFMTJs) [50–54]. It was shown that AFM metals supporting nonrelativistic longitudinal spin-polarized currents driven by strong exchange interactions, rather than relatively weak spin-orbit coupling (SOC), can serve as an efficient spin source similar to ferromagnets or heavy metals, to exert a dampinglike STT on antiferromagnets [36,37,55–60]. This dampinglike STT can generate a persistent ultrafast oscillation under an applied driving current, which is promising for THz applications [55].

It is not obvious, however, how to use the advantages of such a uniformly polarized spin current to deterministically switch the Néel vector of an antiferromagnet.

Such switching typically requires a uniform fieldlike spin torque powered by a staggered spin polarization on AFM sublattices [12,21–23,58], where the driving current is globally spin neutral rather than uniformly spin polarized. So far, the Néel spin torques have only been expected due to SOC in bulk antiferromagnets with a combined $\hat{P}\hat{T}$ symmetry (where $\hat{P}$ is inversion symmetry and $\hat{T}$ is time reversal symmetry) [10,24,25]. It would be desirable to use the advantages of much stronger (compared to a relatively weak SOC) exchange interactions in AFM metals to generate a Néel STT in AFMTJs desirable for high-density applications. This opportunity can be realized using Néel spin currents which have been previously overlooked but appear to occur in most AFM metals, as we demonstrate in this Letter.

Recently, it was predicted that globally spin-neutral currents can generate prominent spin-dependent transport phenomena in AFMTJs, such as the TMR [50] and tunneling anomalous Hall effects (TAHE) [61]. These phenomena rely on the nonrelativistic exchange interactions in the bulk of AFM metals and their strengths are comparable to these in ferromagnetic systems. Importantly, these effects are robust against disorder and interface roughness, contrary to the previous predictions of TMR and STT in AFMTJs [62–67] hindered by disorder [68,69].

In this Letter, we predict that the globally spin-neutral currents responsible for the previously discovered TMR and TAHE in AFMTJs are composed of staggered spin currents on two magnetic sublattices, which we dub the Néel spin currents. We show that the Néel spin currents are also efficient in producing of a robust and strong STT in AFMTJs. Based on symmetry analyses in real space, we find that the Néel spin currents are widely supported in AFM metals. Using first-principles quantum transport calculations [70], we predict strong Néel spin currents in RuO_2, an antiferromagnet with a spin-split Fermi surface, and Fe_4GeTe_2, an antiferromagnet with a spin-degenerate Fermi surface, and demonstrate a sizable field-like STT capable of the deterministic switching of the Néel vector in AFMTJs.

We consider a collinear AFM metal that consists of two magnetic sublattices m_α, where α is the sublattice index, A or B (Fig. 1). A bias voltage (V_b) applied to this antiferromagnet generates a charge current J composed of currents $J_{\alpha\beta}$ flowing through intrasublattice ($\alpha = \beta$) and inter-sublattice ($\alpha \neq \beta$) so that

$$J_{\alpha\beta} = J^{\uparrow}_{\alpha\beta} + J^{\downarrow}_{\alpha\beta}, \tag{1}$$

where $\uparrow$ and $\downarrow$ denote the two spin channels. The associated spin current $J^s_{\alpha\beta}$ is

$$J^s_{\alpha\beta} = J^{\uparrow}_{\alpha\beta} - J^{\downarrow}_{\alpha\beta}. \tag{2}$$

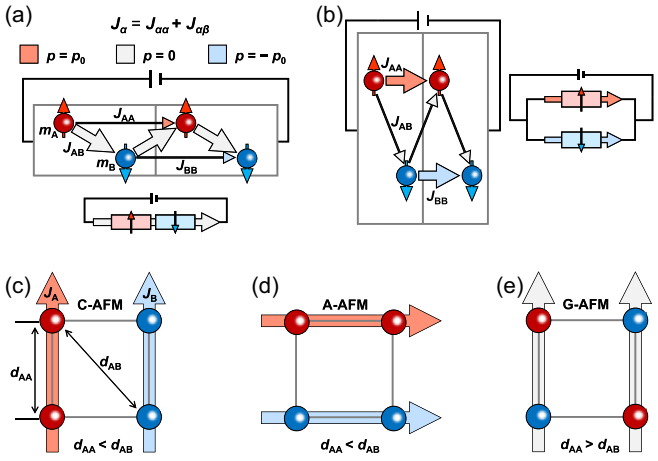

FIG. 1. (a) Schematics of a collinear AFM metal composed of sublattices A and B, where intrasublattice distance d_{AA} is larger than intersublattice distance d_{AB}. In this case, the intrasublattice coupling is weak, and the antiferromagnet can be considered as a resistor with the two sublattices connected in series, where no spin current is flowing through each sublattice. (b) The same as (a) except $d_{AA} < d_{AB}$. In this case, the intersublattice coupling is weak, and the antiferromagnet can be considered as a resistor with the two sublattices connected in parallel, supporting a staggered Néel spin current. (c)–(e) Schematics of the Néel spin currents in C-type (c), A-type (d), and G-type (e) antiferromagnets.

The related conductance $g_{\alpha\beta}$ and spin conductance $g^s_{\alpha\beta}$ are

$$g^{(s)}_{\alpha\beta} = J^{(s)}_{\alpha\beta}/V_b. \tag{3}$$

The $g^s_{\alpha\beta}$ is controlled by a symmetry operation $\hat{O}$ that connects the two magnetic sublattices. For compensated antiferromagnets with $\hat{P}\hat{T}$ symmetry, we obtain $\hat{P}\hat{T}\, g^s_{AA} = -g^s_{BB}$ and $\hat{P}\hat{T}\, g^s_{AB} = -g^s_{AB} = 0$. Therefore, in $\hat{P}\hat{T}$ symmetric antiferromagnets, despite globally spin-neutral currents, staggered intrasublattice spin currents are allowed (due to $J^s_{AA} = -J^s_{BB}$), while intersublattice spin currents are not (due to $J^s_{AB} = 0$). This observation is also valid for antiferromagnets compensated by combined $\hat{T}\hat{t}$ symmetry, where $\hat{t}$ is half a unit cell translation.

$\hat{O}$ can also be crystal symmetry, such as a mirror (glide) reflection or a rotation (screw rotation). For example, in a transport direction parallel to a mirror plane $\hat{M}$, $J^{(s)}_{\alpha\beta}$ represents a longitudinal $J^{(s)}_{\alpha\beta\parallel}$ current parallel to $\hat{M}$ or a transverse $J^{(s)}_{\alpha\beta\perp}$ current perpendicular to $\hat{M}$, with the related spin-conductance components $g^{(s)}_{\alpha\beta\parallel}$ and $g^{(s)}_{\alpha\beta\perp}$. Similarly, we find that $\hat{M}$ enforces $\hat{M}g^s_{AA\parallel} = -g^s_{BB\parallel}$, $\hat{M}g^s_{AB\parallel} = -g^s_{AB\parallel} = 0$, $\hat{M}g^s_{AA\perp} = g^s_{BB\perp}$, and $\hat{M}g^s_{AB\perp} = g^s_{AB\perp}$. These relations imply the presence of a globally spin-neutral longitudinal current $J_\parallel$ that involves an intrasublattice staggered longitudinal

spin current $J^s_{\mathrm{AA}\parallel} = -J^s_{\mathrm{BB}\parallel}$ and a global transverse spin current $J^s_\perp = \sum_{\alpha,\beta} J^s_{\alpha\beta\perp}$. This symmetry analysis in real space is consistent with that previously performed in k space [37,50]. In particular, it explains the presence of the transverse spin current in RuO_2 for an electric field applied along [100], where there is only one mirror plane parallel to this direction [37,41–43], and its absence for an electric field applied along [001], where there are multiple mirror planes parallel to this direction [50,61]. Likewise, a global longitudinal spin current $J^s_\parallel$ is expected, if it does not have the symmetry constraints of $\hat{O}$ [37].

The longitudinal Néel spin current through the magnetic sublattice α is given by

$$J^s_{\alpha\parallel} = \sum_\beta J^s_{\alpha\beta\parallel}. \tag{4}$$

This current is, in general, spin polarized with the spin polarization $p_{\alpha\parallel}$ defined by

$$p_{\alpha\parallel} = \frac{\sum_\beta J^s_{\alpha\beta\parallel}}{\sum_\beta J_{\alpha\beta\parallel}} = \frac{\sum_\beta g^s_{\alpha\beta\parallel}}{\sum_\beta g_{\alpha\beta\parallel}}. \tag{5}$$

When $g^s_{\mathrm{AB}\parallel} = 0$, the magnitude of $p_{\alpha\parallel}$ is determined by the relative values of $g_{\mathrm{AB}\parallel}$ and $g_{\mathrm{AA}\parallel}$ ($g_{\mathrm{BB}\parallel}$). Qualitatively, these conductances are determined by the inter- and intrasublattice couplings (hoppings) that are related to the nearest inter- and intrasublattice distances along the transport direction. When the intersublattice distance (d_{AB}) is much smaller than the intrasublattice distance (d_{AA}) [Fig. 1(a)], the intersublattice coupling dominates, leading to a large $g_{\mathrm{AB}\parallel}$ and hence small $p_{\alpha\parallel}$. In this case, the two AFM sublattices can be considered as being connected in a series with no spin current flowing through each sublattice. On the other hand, if d_{AA} is much smaller than d_{AB} [Fig. 1(b)], a small $g_{\mathrm{AB}\parallel}$ and hence large $p_{\alpha\parallel}$ are expected. In this case, the two AFM sublattices are connected parallel supporting a Néel spin current.

Figures 1(c)–1(e) illustrate typical AFM configurations for simple cubic systems. For C-type antiferromagnets composed of antiparallel-aligned ferromagnetic chains [Fig. 1(c)] and A-type antiferromagnets composed of antiparallel-aligned ferromagnetic layers [Fig. 1(d)], $d_{\mathrm{AA}} < d_{\mathrm{AB}}$ when the transport direction is parallel to the chains (layers), and thus Néel spin currents with sizable $p_{\alpha\parallel}$ are expected in this direction. On the other hand, the checker-board-like magnetic order of G-type antiferromagnets resulting in $d_{\mathrm{AA}} > d_{\mathrm{AB}}$ [Fig. 1(e)] is not supportive to Néel spin currents.

To demonstrate a possibility of a strong Néel spin current, we consider the recently discovered high temperature antiferromagnet RuO_2 [81]. In its rutile structure, the ferromagnetically ordered Ru_A and Ru_B chains along the [001] direction are aligned antiparallel with a large interchain distance [Fig. 2(a)]. Its magnetic space group $P4'_2/mnm'$ does not include $\hat{P}\hat{T}$ and $\hat{T}\hat{t}$ symmetries, but has two glide planes $\hat{M}_x$ and $\hat{M}_y$ perpendicular to the [100] and [010] directions, respectively, connecting the two sublattices Ru_A and Ru_B. This results in the spin-split electronic structure of RuO_2 [82], generating sizable in-plane spin currents and associated spin-torques [37,41–43], a giant TMR [50], and an anomalous Hall effect (if its Néel vector is rotated away from the easy axis) [30].

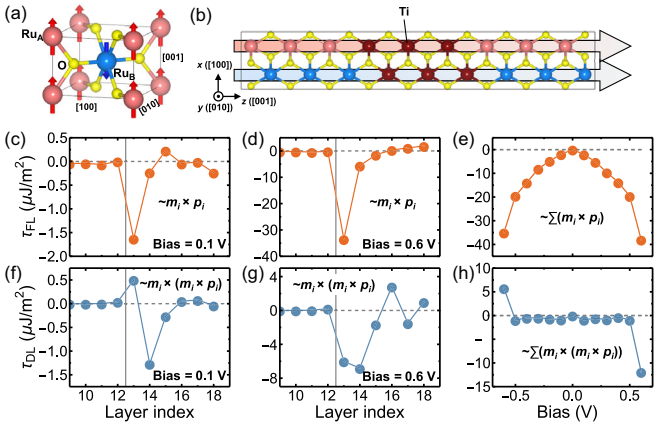

FIG. 2. (a) The atomic structure of RuO_2. (b) The atomic structure of the $RuO_2/TiO_2/RuO_2$ supercell. (c)–(e) The layer resolved fieldlike STT for $V_b = 0.1$ (c) and $V_b = 0.6$ V (d) and the total fieldlike STT (e) in the right half of the $RuO_2/TiO_2/RuO_2$ AFMTJ. (f)–(h) The same as (c)–(e) for the dampinglike STT. The vertical gray lines in (c),(d),(f),(g) denote the interface between TiO_2 and RuO_2.

For V_b applied along the [001] direction, a Néel spin current emerges in RuO_2, due to both $\hat{M}_x$ and $\hat{M}_y$ being parallel to [001]. $d_{\mathrm{AB}}/d_{\mathrm{AA}} = 1.14$ indicates a stronger intrasublattice coupling, resulting in the Néel spin current with estimated $p_{\alpha\parallel} = 35\%$ [70,83] that is comparable to the transport spin polarization of conventional ferromagnetic metals such as Fe, Co, and Ni [84–86]. This spin polarization is responsible for the predicted TMR in an AFMTJ based on RuO_2 electrodes [50].

The sizable $p_{\alpha\parallel}$ in RuO_2 also promises a strong STT [5,7]. To demonstrate this, we build an AFMTJ with RuO_2 (001) electrodes and a TiO_2 (001) insulating barrier layer. Figure 2(b) shows the atomic structure of the $RuO_2/TiO_2/RuO_2$ (001) supercell, which is used in our quantum-transport calculations and includes 6 RuO_2 layers on each side of the AFMTJ separated by 6 TiO_2 layers. To calculate STT exerted on the magnetic moments in the right electrode by the current from the left electrode, we assume that the Néel vectors are along the [100] and [001] directions in the left and right electrodes, respectively [87,88]. Figures 2(c) and 2(f) show the calculated layer-resolved fieldlike STT $\tau_{\mathrm{FL},i}$ and dampinglike STT $\tau_{\mathrm{DL},i}$ in the right half of the junction for a small $V_b = 0.1$ V. We find that $\tau_{\mathrm{FL},i}$ and $\tau_{\mathrm{DL},i}$ are large at the interfacial RuO_2 layers and

then decrease rapidly at the layers away from the interface. This is consistent with the known behavior of STTs in MTJs [89]. Interestingly, $\tau_{\mathrm{FL},i}$ and $\tau_{\mathrm{DL},i}$ exhibit distinct behaviors: while $\tau_{\mathrm{FL},i}$ for the first two interfacial layers are parallel, $\tau_{\mathrm{DL},i}$ are antiparallel (staggered), indicating that the STTs are generated by the staggered spin polarization $p_{\mathrm{A}\parallel} = -p_{\mathrm{B}\parallel}$ of the Néel spin current. As a result, for the low V_b, the total τ_{FL} is large, while the total τ_{DL} is small [Figs. 2(e) and 2(h)].

For a large $V_b = 0.6$ V, both $\tau_{\mathrm{FL},i}$ and $\tau_{\mathrm{DL},i}$ are enhanced. In particular, we find that $\tau_{\mathrm{DL},i}$ at the two interfacial layers become parallel. This is due to an additional uniform spin current with spin polarization p_U generated by the uncompensated interfacial moments. Nevertheless, the total τ_{DL} remains small due to the most $\tau_{\mathrm{DL},i}$ being staggered. On the contrary, the total τ_{FL} is strongly enhanced and becomes comparable to that calculated for an Fe/MgO/Fe MTJ with similar barrier thickness [90]. Importantly, we find that independent of the interfacial configurations, τ_{FL} remains much stronger than τ_{DL}, indicating the dominant role of the bulk Néel spin current for STT [70]. This fact implies that the STT should be robust against interface roughness.

Next, we consider a different type of AFM metal, namely, the recently discovered two-dimensional (2D) van der Waals magnet Fe_4GeTe_2, where the AFM order is introduced by doping [91]. A monolayer Fe_4GeTe_2 contains seven atomic layers stacked with a Te-Fe-Fe-Ge-Fe-Fe-Te sequence and Fe moments coupled ferromagnetically [Fig. 3(a)]. A bilayer Fe_4GeTe_2 has two AFM ordered monolayers. It has $\hat{P}\hat{T}$ symmetry and hence Kramers degeneracy of its band structure [Fig. 3(b)]. Such antiferromagnets are considered to host a hidden spin polarization [92]. The bilayer Fe_4GeTe_2 has a large $d_{\mathrm{AB}}/d_{\mathrm{AA}} > 2.82$, indicating a very weak intersublattice coupling. For the transport along the in-plane $[1\bar{1}0]$ direction, we predict a Néel spin current with a large spin polarization $p_{\alpha\parallel} = 68\%$.

In order to illustrate possible spin-dependent transport phenomena driven by the Néel spin currents in such spin-degenerate antiferromagnets, we build two artificial AFMTJs (denoted as FGT|GeTe|FGT and FGT|□|FGT) with Fe_4GeTe_2 $(1\bar{1}0)$ electrodes, and use GeTe molecules as the barrier for FGT|GeTe|FGT [Fig. 3(c)] and a vacuum layer (denoted by □) of ~4 Å for FGT|□|FGT [Fig. 3(d)]. Figures 3(e) and 3(f) show the calculated transmissions of these AFMTJs as functions of energy for parallel (P) and antiparallel (AP) states of the Néel vector. We find that independent of the energy and the barrier, the total transmission is always larger for the P state (T_P) than for the AP state (T_{AP}) in the calculated energy window. At the Fermi energy (E_F), the TMR ratio $(T_P - T_{AP})/T_{AP}$ is ~93% for FGT|GeTe|FGT AFMTJ and ~24% for FGT|□|FGT AFMTJ [Fig. 3(g)]. These sizable TMR values are

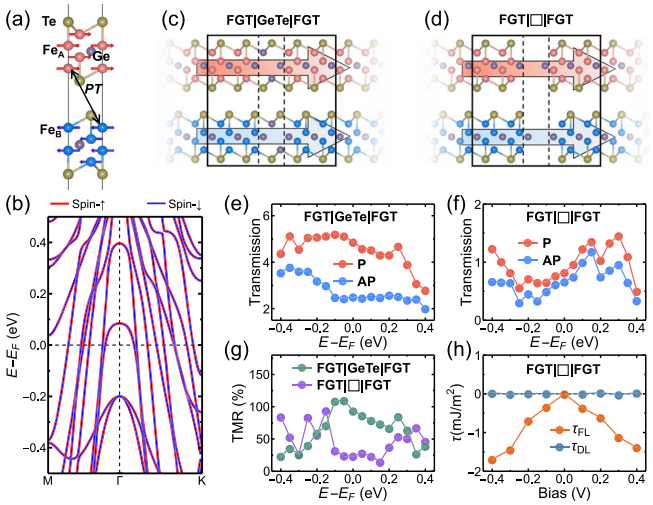

FIG. 3. (a),(b) The atomic structure (a) and band structure (b) of an Fe_4GeTe_2 bilayer. (c),(d) The supercells used for FGT|GeTe|FGT (c) and FGT|□|FGT (d) AFMTJs. (e),(f) The transmissions of FGT|GeTe|FGT (e) and FGT|□|FGT (f) AFMTJs for the P and AP states as a function of energy. (g) The TMR ratio for FGT|GeTe|FGT and FGT|□|FGT AFMTJs as a function of energy. (h) The total fieldlike and dampinglike STTs in the right electrode of FGT|□|FGT AFMTJ as a function of bias voltage.

unexpected since the Fermi surfaces of the electrodes are spin degenerate for the P and AP states. On the other hand, it can be qualitatively understood by Julliere's formula $TMR = [2p_{\alpha\parallel}^2/(1 - p_{\alpha\parallel}^2)]$ [2,3] with the large $p_{\alpha\parallel}$, indicating that this spin neutral AFMTJ can be qualitatively considered as two MTJs connected in parallel. Figure 3(h) shows the calculated STT for this AFMTJ. We find a large τ_{FL} and negligible τ_{DL}, due to the staggered spin polarizations in the Néel spin currents.

Finally, we show that the Néel spin currents are crucial for the deterministic switching of the Néel vector in antiferromagnets. We perform a macroscopic spin dynamics simulation in an antiferromagnet with a z-directional anisotropy field $H_K = 0.1$ T, an exchange field $H_{\mathrm{ex}} = 100$ T, and a damping parameter $\mu = 0.01$. A current is applied to generate an effective field H_α in sublattice α and hence $\tau_{\mathrm{FL},\alpha}$ and $\tau_{\mathrm{DL},\alpha}$ for switching. If there are only perfect staggered Néel spin currents, H_α is staggered as $H_{\mathrm{A}} = -H_B = H_N$. A uniform spin current contributed by the interface generates an additional effective field H_U and influences H_α as $H_A = H_N + H_U$ and $H_B = -H_N + H_U$. In this case, $\tau_{\mathrm{FL},\alpha}$ and $\tau_{\mathrm{DL},\alpha}$ can be decomposed to uniform $\tau_{\mathrm{FL}N,\alpha}$ and staggered $\tau_{\mathrm{DL}N,\alpha}$ driven by the Néel spin currents, and staggered $\tau_{\mathrm{FL}U,\alpha}$ and uniform $\tau_{\mathrm{DL}U,\alpha}$ driven by the uniform spin currents.

We fix $H_N = 0.2$ T and change the magnitude of H_U in the simulation. In the absence of H_U, we find that the Néel vector initially pointing along the $+z$ direction is rapidly reversed in a few ps [Fig. 4(a)], indicating an ultrafast

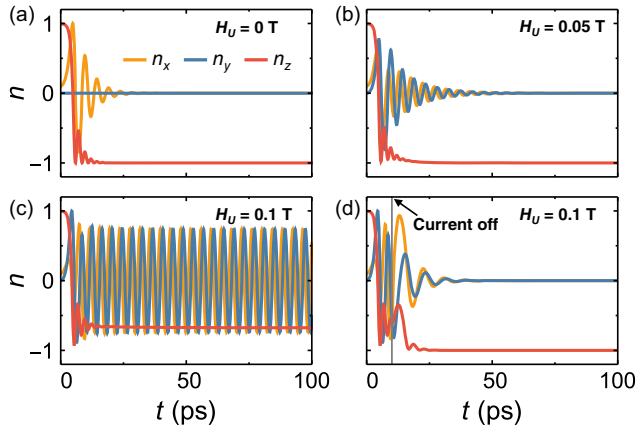

FIG. 4. The simulated dynamics of the x, y, and z components of the Néel vector under the current induced effective fields $H_A = H_N + H_U$ and $H_B = -H_N + H_U$. (a) $H_N = 0.2$ and $H_U = 0$ T. (b) $H_N = 0.2$ and $H_U = 0.05$ T. (c) $H_N = 0.2$ and $H_U = 0.1$ T. (d) $H_N = 0.2$ and $H_U = 0.1$ T for the first 10 ps and then $H_N = H_U = 0$.

deterministic switching induced by the Néel spin currents. We also perform the simulation solely with $\tau_{\mathrm{FL}N,\alpha}$ or staggered $\tau_{\mathrm{DL}N,\alpha}$, and confirm that the uniform $\tau_{\mathrm{FL}N,\alpha}$ is responsible for the switching [70]. For a small $H_U = 0.05$ T, $\tau_{\mathrm{DL}U,\alpha}$ induces an oscillation of the Néel vector which gradually decays during the current application [Fig. 4(b)]. This leads to a longer time for the full switching of the Néel vector. For a larger $H_U = 0.1$ T, we find that the oscillation is persistent and hence the full switching of the Néel vector cannot be realized by a constant current [Fig. 4(c)], indicating the dominant role of $\tau_{\mathrm{DL}U,\alpha}$ in this case. We note, however, that the z component of the Néel vector keeps being negative during the oscillation because of $\tau_{\mathrm{FL}N,\alpha}$. Therefore, if we apply a short current pulse [10 ps as shown in Fig. 4(c)], the Néel vector will first oscillate and then rapidly relax to the $-z$ direction after the pulse ended. These simulations clearly prove the decisive role of the Néel spin currents in the deterministic Néel vector switching.

The STT and TMR, serving as the evidence of the Néel spin currents, are feasible in experiment. Especially, epitaxial films of AFM RuO_2 have been grown experimentally [30,41–43], promising for the high-quality RuO_2-based AFMTJs. The recently developed edge-epitaxy techniques allow fabricating AFMTJs based on lateral heterostructures using the A-type 2D AFM metals such as Fe_4GeTe_2 [93–95]. Moreover, the Néel spin currents are also expected to generate self-torque in these materials in the presence of the asymmetric boundary conditions. This is analogous to the self-torque driven by a uniform spin current in a single ferromagnet [96,97], and is particularly useful for the AFM spintronics based on a single antiferromagnet [61].

In practice, the factor d_{AB}/d_{AA} can serve as a simple measure of the Néel spin current strength. We note that some antiferromagnets with a large d_{AB}/d_{AA} might be insulating. While, in this case, generating the Néel spin currents by an electric field is difficult, it is possible to use thermoelectric or photogalvanic effects to produce Néel spin currents. This opens new opportunities for spin caloritronics [98] and optospintronics [99] based on insulating antiferromagnets. The Néel spin currents can be also promising in conventional spintronics to separate spin currents of two sublattices. For example, attaching an AFM bilayer Fe_4GeTe_2 to the top of a nonmagnetic material can serve as a contact in a spin transistor, where only the Néel spin current at the bottom layer is injected into the transistor.

In conclusion, we have predicted that the spin-neutral current in antiferromagnets is composed of staggered spin currents on two magnetic sublattices, dubbed the Néel spin current. The concept of the Néel spin current provides a new insight into the electronic transport in antiferromagnets and helps reveal new physics important for spintronic applications. We demonstrate that the presence of the Néel spin currents is responsible for the emergence of giant TMR and a sizable fieldlike STT capable of the deterministic switching of the Néel vector in AFMTJs. Overall, our work uncovers a previously unexplored potential of antiferromagnets, and paves a new route to realize efficient reading and writing of the Néel vector for antiferromagnetic spintronics.

We thank Qihang Liu, Jinsong Zhang, and Bo Li for helpful discussions. This work was supported by the National Key Research and Development Program of China (Grants No. 2021YFA1600200, No. 2022YFA1403203), the National Science Foundation of China (NSFC Grants No. 12241405, No. 12274411, No. 52250418, No. 12174019, No. 12274412, No. 12274115, No. 12204009, No. U2032215), and the Program for Science & Technology Innovation Talents in Universities of Henan Province (No. 23HASTIT027). The calculations were performed at Hefei Advanced Computing Center. The figures were created using the SciDraw scientific figure preparation system [100].

*These authors contributed equally to this work.
†dfshao@issp.ac.cn
‡tsymbal@unl.edu

[1] *Spintronics Handbook: Spin Transport and Magnetism*, 2nd ed., edited by E. Y. Tsymbal and I. Žutić (CRC Press, Boca Raton, 2019).
[2] M. Julliere, Tunneling between ferromagnetic films, Phys. Lett. **54A**, 225 (1975).
[3] E. Y. Tsymbal, O. N. Mryasov, and P. R. LeClair, Spin-dependent tunneling in magnetic tunnel junctions, J. Phys. Condens. Matter **15**, R109 (2003).
[4] J. S. Moodera, L. R. Kinder, T. M. Wong, and R. Meservey, Large Magnetoresistance at Room Temperature in Ferromagnetic Thin Film Tunnel Junctions, Phys. Rev. Lett. **74**, 3273 (1995).

[5] J. C. Slonczewski, Current-driven excitation of magnetic multilayers, J. Magn. Magn. Mater. **159**, L1 (1996).

[6] A. Brataas, A. D. Kent, and H. Ohno, Current-induced torques in magnetic materials, Nat. Mater. **11**, 372 (2012).

[7] D. Ralph and M. Stiles, Spin transfer torques, J. Magn. Magn. Mater. **320**, 1190 (2008).

[8] A. V. Khvalkovskiy, D. Apalkov, S. Watts, R. Chepulskii, R. S. Beach, A. Ong, X. Tang, A. Driskill-Smith, W. H. Butler, P. B. Visscher, D. Lottis, E. Chen, V. Nikitin, and M. Krounbi, Basic principles of STT-MRAM cell operation in memory arrays, J. Phys. D **46**, 074001 (2013).

[9] V. Baltz, A. Manchon, M. Tsoi, T. Moriyama, T. Ono, and Y. Tserkovnyak, Antiferromagnetic spintronics, Rev. Mod. Phys. **90**, 015005 (2018).

[10] T. Jungwirth, X. Marti, P. Wadley, and J. Wunderlich, Antiferromagnetic spintronics, Nat. Nanotechnol. **11**, 231 (2016).

[11] T. Jungwirth, J. Sinova, A. Manchon, X. Marti, J. Wunderlich, and C. Felser, The multiple directions of antiferromagnetic spintronics, Nat. Phys. **14**, 200 (2018).

[12] J. Železný, P. Wadley, K. Olejník, A. Hoffmann, and H. Ohno, Spin transport and spin torque in antiferromagnetic devices, Nat. Phys. **14**, 220 (2018).

[13] X. Zhang, Q. Liu, J.-W. Luo, A. J. Freeman, and A. Zunger, Hidden spin polarization in inversion-symmetric bulk crystals, Nat. Phys. **10**, 387 (2014).

[14] S. Hayami, Y. Yanagi, and H. Kusunose, Momentum-dependent spin splitting by collinear antiferromagnetic ordering, J. Phys. Soc. Jpn. **88**, 123702 (2019).

[15] L.-D. Yuan, Z. Wang, J.-W. Luo, E. I. Rashba, and A. Zunger, Giant momentum-dependent spin splitting in centrosymmetric low-Z antiferromagnets, Phys. Rev. B **102**, 014422 (2020).

[16] L.-D. Yuan, Z. Wang, J.-W. Luo, and A. Zunger, Prediction of low-Z collinear and noncollinear antiferromagnetic compounds having momentum-dependent spin splitting even without spin-orbit coupling, Phys. Rev. Mater. **5**, 014409 (2021).

[17] S. Hayami, Y. Yanagi, and H. Kusunose, Bottom-up design of spin-split and reshaped electronic band structures in antiferromagnets without spin-orbit coupling: Procedure on the basis of augmented multipoles, Phys. Rev. B **102**, 144441 (2020).

[18] P. Liu, J. Li, J. Han, X. Wan, and Q. Liu, Spin-Group Symmetry in Magnetic Materials with Negligible Spin-Orbit Coupling, Phys. Rev. X **12**, 021016 (2022).

[19] L. Šmejkal, J. Sinova, and T. Jungwirth, Beyond Conventional Ferromagnetism and Antiferromagnetism: A Phase with Nonrelativistic Spin and Crystal Rotation Symmetry, Phys. Rev. X **12**, 031042 (2022).

[20] I. I. Mazin, K. Koepernik, M. D. Johannes, R. González-Hernández, and L. Smejkal, Prediction of unconventional magnetism in doped $FeSb_2$, Proc. Natl. Acad. Sci. U.S.A. **118**, e2108924118 (2021).

[21] J. Železný, H. Gao, K. Výborný, J. Zemen, J. Mašek, A. Manchon, J. Wunderlich, J. Sinova, and T. Jungwirth, Relativistic Néel-Order Fields Induced by Electrical Current in Antiferromagnets, Phys. Rev. Lett. **113**, 157201 (2014).

[22] J. Železný, H. Gao, A. Manchon, F. Freimuth, Y. Mokrousov, J. Zemen, J. Mašek, J. Sinova, and T. Jungwirth, Spin-orbit torques in locally and globally noncentrosymmetric crystals: Anti-ferromagnets and ferromagnets, Phys. Rev. B **95**, 014403 (2017).

[23] A. Manchon, J. Zelezný, I. M. Miron, T. Jungwirth, J. Sinova, A. Thiaville, K. Garello, and P. Gambardella, Current-induced spin-orbit torques in ferromagnetic and antiferromagnetic systems, Rev. Mod. Phys. **91**, 035004 (2019).

[24] P. Wadley *et al.*, Electrical switching of an antiferromagnet, Science **351**, 587 (2016).

[25] X. F. Zhou, J. Zhang, F. Li, X. Z. Chen, G. Y. Shi, Y. Z. Tan, Y. D. Gu, M. S. Saleem, H. Q. Wu, F. Pan, and C. Song, Strong Orientation-Dependent Spin-Orbit Torque in Thin Films of the Antiferromagnet Mn_2Au, Phys. Rev. Appl. **9**, 054028 (2018).

[26] N. Nagaosa, J. Sinova, S. Onoda, A. H. MacDonald, and N. P. Ong, Anomalous Hall effect, Rev. Mod. Phys. **82**, 1539 (2010).

[27] H. Chen, Q. Niu, and A. H. MacDonald, Anomalous Hall Effect Arising from Noncollinear Antiferromagnetism, Phys. Rev. Lett. **112**, 017205 (2014).

[28] S. Nakatsuji, N. Kiyohara, and T. Higo, Large anomalous Hall effect in a non-collinear antiferromagnet at room temperature, Nature (London) **527**, 212 (2015).

[29] L. Šmejkal, R. González-Hernández, T. Jungwirth, and J. Sinova, Crystal Hall effect in collinear antiferromagnets, Sci. Adv. **6**, eaaz8809 (2020).

[30] Z. Feng, X. Zhou, L. Šmejkal, L. Wu, Z. Zhu, H. Guo, R. González-Hernández, X. Wang, H. Yan, P. Qin, X. Zhang, H. Wu, H. Chen, C. Jiang, M. Coey, J. Sinova, T. Jungwirth, and Z. Liu, An anomalous Hall effect in altermagnetic ruthenium dioxide, Nat. Electron. Rev. **5**, 735 (2022).

[31] I. Sodemann and L. Fu, Quantum Nonlinear Hall Effect Induced by Berry Curvature Dipole in Time-Reversal Invariant Materials, Phys. Rev. Lett. **115**, 216806 (2015).

[32] Z. Du, H.-Z. Lu, and X. Xie, Nonlinear Hall effects, Nat. Rev. Phys. **3**, 744 (2021).

[33] D.-F. Shao, S.-H. Zhang, G. Gurung, W. Yang, and E. Y. Tsymbal, Nonlinear Anomalous Hall Effect for Néel Vector Detection, Phys. Rev. Lett. **124**, 067203 (2020).

[34] H. Liu, J. Zhao, Y.-X. Huang, W. Wu, X.-L. Sheng, C. Xiao, and S. A. Yang, Intrinsic Second-Order Anomalous Hall Effect and its Application in Compensated Antiferromagnets, Phys. Rev. Lett. **127**, 277202 (2021).

[35] C. Wang, Y. Gao, and D. Xiao, Intrinsic Nonlinear Hall Effect in Antiferromagnetic Tetragonal CuMnAs, Phys. Rev. Lett. **127**, 277201 (2021).

[36] J. Železný, Y. Zhang, C. Felser, and B. Yan, Spin-Polarized Current in Noncollinear Antiferromagnets, Phys. Rev. Lett. **119**, 187204 (2017).

[37] R. González-Hernández, L. Šmejkal, K. Výborný, Y. Yahagi, J. Sinova, T. Jungwirth, and J. Železný, Efficient Electrical Spin-Splitter Based on Nonrelativistic Collinear Antiferromagnetism, Phys. Rev. Lett. **126**, 127701 (2021).

[38] D.-F. Shao, G. Gurung, S.-H. Zhang, and E. Y. Tsymbal, Dirac Nodal Line Metal for Topological Antiferromagnetic Spintronics, Phys. Rev. Lett. **122**, 077203 (2019).

[39] Y. Zhang, Y. Sun, H. Yang, J. Železný, S. P. P. Parkin, C. Felser, and B. Yan, Strong anisotropic anomalous Hall effect and spin Hall effect in the chiral antiferromagnetic compounds Mn_3X (X = Ge, Sn, Ga, Ir, Rh, and Pt), Phys. Rev. B **95**, 075128 (2017).

[40] T. Nan *et al.*, Controlling spin current polarization through non-collinear antiferromagnetism, Nat. Commun. **11**, 4671 (2020).

[41] A. Bose, N. J. Schreiber, R. Jain, D.-F. Shao, H. P. Nair, J. Sun, X. S. Zhang, D. A. Muller, E. Y. Tsymbal, D. G. Schlom, and D. C. Ralph, Tilted spin current generated by the collinear antiferromagnet ruthenium dioxide, Nat. Electron. Rev. **5**, 267 (2022).

[42] H. Bai, L. Han, X. Y. Feng, Y. J. Zhou, R. X. Su, Q. Wang, L. Y. Liao, W. X. Zhu, X. Z. Chen, F. Pan, X. L. Fan, and C. Song, Observation of Spin Splitting Torque in a Collinear Antiferromagnet RuO_2, Phys. Rev. Lett. **128**, 197202 (2022).

[43] S. Karube, T. Tanaka, D. Sugawara, N. Kadoguchi, M. Kohda, and J. Nitta, Observation of Spin-Splitter Torque in Collinear Antiferromagnetic RuO_2, Phys. Rev. Lett. **129**, 137201 (2022).

[44] X. Chen, S. Shi, G. Shi, X. Fan, C. Song, X. Zhou, H. Bai, L. Liao, Y. Zhou, H. Zhang, A. Li, Y. Chen, X. Han, S. Jiang, Z. Zhu, H. Wu, X. Wang, D. Xue, H. Yang, and F. Pan, Observation of the antiferromagnetic spin Hall effect, Nat. Mater. **20**, 800 (2021).

[45] L. Huang, Y. Zhou, H. Qiu, H. Bai, C. Chen, W. Yu, L. Liao, T. Guo, F. Pan, B. Jin, and C. Song, Antiferromagnetic inverse spin Hall effect, Adv. Mater. **34**, 2205988 (2022).

[46] G. Gurung, D.-F. Shao, and E. Y. Tsymbal, Transport spin polarization of noncollinear antiferromagnetic antiperovskites, Phys. Rev. Mater. **5**, 124411 (2021).

[47] S. Hu, D.-F. Shao, H. Yang, C. Pan, Z. Fu, M. Tang, Y. Yang, W. Fan, S. Zhou, E. Y. Tsymbal, and X. Qiu, Efficient perpendicular magnetization switching by a magnetic spin Hall effect in a noncollinear antiferromagnet, Nat. Commun. **13**, 4447 (2022).

[48] D. Go, M. Sallermann, F. R. Lux, S. Blügel, O. Gomonay, and Y. Mokrousov, Noncollinear Spin Current for Switching of Chiral Magnetic Textures, Phys. Rev. Lett. **129**, 097204 (2022).

[49] H. Bai, Y. C. Zhang, L. Han, Y. J. Zhou, F. Pan, and C. Song, Antiferromagnetism: An efficient and controllable spin source, Appl. Phys. Rev. **9**, 041316 (2022).

[50] D.-F. Shao, S. H. Zhang, M. Li, C. B. Eom, and E. Y Tsymbal, Spin-neutral currents for spintronics, Nat. Commun. **12**, 7061 (2021).

[51] L. Šmejkal, A. Birk Hellenes, R. González-Hernández, J. Sinova, and T. Jungwirth, Giant, and Tunneling Magnetoresistance in Unconventional Collinear Antiferromagnets with Nonrelativistic Spin-Momentum Coupling, Phys. Rev. X **12**, 011028 (2022).

[52] J. Dong, X. Li, G. Gurung, M. Zhu, P. Zhang, F. Zheng, E. Y. Tsymbal, and J. Zhang, Tunneling Magnetoresistance in Noncollinear Antiferromagnetic Tunnel Junctions, Phys. Rev. Lett. **128**, 197201 (2022).

[53] P. Qin, H. Yan, X. Wang, H. Chen, Z. Meng, J. Dong, M. Zhu, J. Cai, Z. Feng, X. Zhou, L. Liu, T. Zhang, Z. Zeng, J. Zhang, C. Jiang, and Z. Liu, Room-temperature magnetoresistance in an all-antiferromagnetic tunnel junction, Nature (London) **613**, 485 (2023).

[54] X. Chen, T. Higo, K. Tanaka, T. Nomoto, H. Tsai, H. Idzuchi, M. Shiga, S. Sakamoto, R. Ando, H. Kosaki, T. Matsuo, D. Nishio-Hamane, R. Arita, S. Miwa, and S. Nakatsuji, Octupole-driven magnetoresistance in an antiferromagnetic tunnel junction, Nature (London) **613**, 490 (2023).

[55] R. Cheng, M. W. Daniels, J.-G. Zhu, and D. Xiao, Ultrafast switching of antiferromagnets via spin-transfer torque, Phys. Rev. B **91**, 064423 (2015).

[56] G. Gurung, D.-F. Shao, and E. Y. Tsymbal, Spin-torque switching of noncollinear antiferromagnetic antiperovskites, Phys. Rev. B **101**, 140405(R) (2020).

[57] O. V. Gomonay and V. M. Loktev, Spin transfer and current-induced switching in antiferromagnets, Phys. Rev. B **81**, 144427 (2010).

[58] O. Gomonay, V. Baltz, A. Brataas, and Y. Tserkovnyak, Antiferromagnetic spin textures and dynamics, Nat. Phys. **14**, 213 (2018).

[59] X. Z. Chen, R. Zarzuela, J. Zhang, C. Song, X. F. Zhou, G. Y. Shi, F. Li, H. A. Zhou, W. J. Jiang, F. Pan, and Y. Tserkovnyak, Antidamping-Torque-Induced Switching in Biaxial Antiferromagnetic Insulators, Phys. Rev. Lett. **120**, 207204 (2018).

[60] S. Ghosh, A. Manchon, and J. Železný, Unconventional Robust Spin-Transfer Torque in Noncollinear Antiferromagnetic Junctions, Phys. Rev. Lett. **128**, 097702 (2022).

[61] D.-F. Shao, S.-H. Zhang, R.-C. Xiao, Z.-A. Wang, W. J. Lu, Y. P. Sun, and E. Y. Tsymbal, Spin-neutral tunneling anomalous Hall effect, Phys. Rev. B **106**, L180404 (2022).

[62] A. S. Núñez, R. A. Duine, P. Haney, and A. H. MacDonald, Theory of spin torques and giant magnetoresistance in antiferromagnetic metals, Phys. Rev. B **73**, 214426 (2006).

[63] P. M. Haney, D. Waldron, R. A. Duine, A. S. Núñez, H. Guo, and A. H. MacDonald, *Ab initio* giant magnetoresistance and current-induced torques in Cr/Au/Cr multilayers, Phys. Rev. B **75**, 174428 (2007).

[64] Y. Xu, S. Wang, and K. Xia, Spin-Transfer Torques in Antiferromagnetic Metals from First Principles, Phys. Rev. Lett. **100**, 226602 (2008).

[65] P. Merodio, A. Kalitsov, H. Ba, V. Baltz, and M. Chshiev, Spin-dependent transport in antiferromagnetic tunnel junctions, Appl. Phys. Lett. **105**, 122403 (2014).

[66] M. Stamenova, R. Mohebbi, J. Seyed-Yazdi, I. Rungger, and S. Sanvito, First-principles spin-transfer torque in CuMnAGaP|CuMnAs junctions, Phys. Rev. B **95**, 060403 (2017).

[67] H. Saidaoui, A. Manchon, and X. Waintal, Robust spin transfer torque in antiferromagnetic tunnel junctions, Phys. Rev. B **95**, 134424 (2017).

[68] H. B. M. Saidaoui, A. Manchon, and X. Waintal, Spin transfer torque in antiferromagnetic spin valves: From clean to disordered regimes, Phys. Rev. B **89**, 174430 (2014).

[69] A. Manchon, Spin diffusion and torques in disordered antiferromagnets, J. Phys. Condens. Matter **29**, 104002 (2017).

[70] See Supplemental Material at http://link.aps.org/supplemental/10.1103/PhysRevLett.130.216702 for calculation methods, estimation of spin polarizations of Néel spin currents, STT in $RuO_2TiO_2|RuO_2$ AFMTJ with different TiO_2 thickness, dynamics of the Néel vector with only fieldlike or dampinglike STTs, and discussion of mechanism of TMR in magnetic tunnel junctions, which includes Refs. [71–80].
[71] G. Kresse and D. Joubert, From ultrasoft pseudopotentials to the projector augmented-wave method, Phys. Rev. B **59**, 1758 (1999).
[72] G. Kresse and J. Furthmuller, Efficient iterative schemes for *ab initio* total-energy calculations using a plane-wave basis set, Phys. Rev. B **54**, 11169 (1996).
[73] J. P. Perdew, K. Burke, and M. Ernzerhof, Generalized Gradient Approximation Made Simple, Phys. Rev. Lett. **77**, 3865 (1996).
[74] V. I. Anisimov, J. Zaanen, and O. K. Andersen, Band theory and Mott insulators: Hubbard *U* instead of Stoner *I*, Phys. Rev. B **44**, 943 (1991).
[75] S. L. Dudarev, G. A. Botton, S. Y. Savrasov, C. J. Humphreys, and A. P. Sutton, Electron-energy-loss spectra and the structural stability of nickel oxide: An LSDA + U study, Phys. Rev. B **57**, 1505 (1998).
[76] S. Grimme, J. Antony, S. Ehrlich, and H. Krieg, A consistent and accurate *ab initio* parametrization of density functional dispersion correction (DFT-D) for the 94 elements H-Pu, J. Chem. Phys. **132**, 154104 (2010).
[77] J. Taylor, H. Guo, and J. Wang, *Ab initio* modeling of quantum transport properties of molecular electronic devices, Phys. Rev. B **63**, 245407 (2001).
[78] M. Brandbyge, J.-L. Mozos, P. Ordejón, J. Taylor, and K. Stokbro, Density-functional method for nonequilibrium electron transport, Phys. Rev. B **65**, 165401 (2002).
[79] S. Smidstrup *et al.*, QuantumATK: An integrated platform of electronic and atomic-scale modelling tools, J. Phys. Condens. Matter **32**, 015901 (2020).
[80] D. R. Hamann, Optimized norm-conserving Vanderbilt pseudopotentials, Phys. Rev. B **88**, 085117 (2013).
[81] T. Berlijn, P. C. Snijders, O. Delaire, H.-D. Zhou, T. A. Maier, H.-B. Cao, S.-X. Chi, M. Matsuda, Y. Wang, M. R. Koehler, P. R. C. Kent, and H. H. Weitering, Itinerant Antiferromagnetism in RuO_2, Phys. Rev. Lett. **118**, 077201 (2017).
[82] K.-H. Ahn, A. Hariki, K.-W. Lee, and J. Kuneš, RuO_2 Antiferromagnetism in as *d*-wave Pomeranchuk instability, Phys. Rev. B **99**, 184432 (2019).
[83] G. C. Solomon, C. Herrmann, T. Hansen, V. Mujica, and M. A. Ratner, Exploring local currents in molecular junctions, Nat. Chem. **2**, 223 (2010).
[84] R. J. Soulen Jr., J. M. Byers, M. S. Osofsky, B. Nadgorny, T. Ambrose, S. F. Cheng, P. R. Broussard, C. T. Tanaka, J. Nowak, J. S. Moodera, A. Barry, and J. M. D. Coey, Measuring the spin polarization of a metal with a superconducting point contact, Science **282**, 85 (1998).
[85] S. K. Upadhyay, A. Palanisami, R. N. Louie, and R. A. Buhrman, Probing Ferromagnets with Andreev Reflection, Phys. Rev. Lett. **81**, 3247 (1998).
[86] I. I. Mazin, How to Define and Calculate the Degree of Spin Polarization in Ferromagnets, Phys. Rev. Lett. **83**, 1427 (1999).
[87] I. Theodonis, N. Kioussis, A. Kalitsov, M. Chshiev, and W. H. Butler, Anomalous Bias Dependence of Spin Torque in Magnetic Tunnel Junctions, Phys. Rev. Lett. **97**, 237205 (2006).
[88] B. K. Nikolić, K. Dolui, M. D. Petrović, P. Plecháč, T. Markussen, and K. Stokbro, First-principles quantum transport modeling of spin-transfer and spin-orbit torques in magnetic multilayers, in *Handbook of Materials Modeling*, edited by W. Andreoni and S. Yip (Springer, Cham, 2018).
[89] C. Heiliger and M. D. Stiles, *Ab Initio* Studies of the Spin-Transfer Torque in Magnetic Tunnel Junctions, Phys. Rev. Lett. **100**, 186805 (2008).
[90] X. Jia, K. Xia, Y. Ke, and H. Guo, Nonlinear bias dependence of spin-transfer torque from atomic first principles, Phys. Rev. B **84**, 014401 (2011).
[91] J. Seo, E. S. An, T. Park, S.-Y. Hwang, G.-Y. Kim, K. Song, W.-s. Noh, J. Y. Kim, G. S. Choi, M. Choi, E. Oh, K. Watanabe, T. Taniguchi, J.-H. Park, Y. J. Jo, H. W. Yeom, S.-Y. Choi, J. H. Shim, and J. S. Kim, Tunable high-temperature itinerant antiferromagnetism in a van der Waals magnet, Nat. Commun. **12**, 2844 (2021).
[92] W. Chen, M. Gu, J. Li, P. Wang, and Q. Liu, Role of Hidden Spin Polarization in Nonreciprocal Transport of Antiferromagnets, Phys. Rev. Lett. **129**, 276601 (2022).
[93] M.-Y. Li, Y. Shi, C.-C. Cheng, L.-S. Lu, Y.-C. Lin, H. Tang, M. Tsai, C. Chu, K. Wei, J.-h. He, W.-H. Chang, K. Suenaga, and L.-J. Li, Epitaxial growth of a monolayer $WSe_2 - MoS_2$ lateral p–n junction with an atomically sharp interface, Science **349**, 524 (2015).
[94] P. K. Sahoo, S. Memaran, Y. Xin, L. Balicas, and Humberto R. Gutiérrez, One-pot growth of two-dimensional lateral heterostructures via sequential edge-epitaxy, Nature (London) **553**, 63 (2018).
[95] Z. Zhang, P. Chen, X. Duan, K. Zang, J. Luo, and X. Duan, Robust epitaxial growth of two-dimensional heterostructures, multiheterostructures, and superlattices, Science **357**, 788 (2017).
[96] W. Wang, T. Wang, V. P. Amin, Y. Wang, A. Radhakrishnan, A. Davidson, S. R. Allen, T. J. Silva, H. Ohldag, D. Balzar, B. L. Zink, P. M. Haney, J. Q. Xiao, D. G. Cahill, V. O. Lorenz, and X. Fan, Anomalous spin–orbit torques in magnetic single-layer films, Nat. Nanotechnol. **14**, 819 (2019).
[97] D. Cspedes-Berrocal, H. Damas, S. Petit-Watelot, D. Maccariello, P. Tang, A. Arriola-Crdova, P. Vallobra, Y. Xu, J.-L. Bello, E. Martin, S. Migot, J. Ghanbaja, S. Zhang, M. Hehn, S. Mangin, C. Panagopoulos, V. Cros, A. Fert, and J.-C. Rojas-Snchez, Current-induced spin torques on single GdFeCo magnetic layers, Adv. Mater. **33**, 2007047 (2021).
[98] G. E. W. Bauer, E. Saitoh, and B. J. van Wees, Spin caloritronics, Nat. Mater. **11**, 391 (2012).
[99] P. Němec, M. Fiebig, T. Kampfrath, and A. V. Kimel, Antiferromagnetic opto-spintronics, Nat. Phys. **14**, 229 (2018).
[100] M. A. Caprio, LevelScheme: A level scheme drawing and scientific figure preparation system for Mathematica, Comput. Phys. Commun. **171**, 107 (2005).